

Chiral waveguide QED: Strongly correlated photon transport with weakly coupled emitters

Sahand Mahmoodian,^{1, 2} Mantas Čepulkovskis,³ Sumanta Das,³
Peter Lodahl,³ Klemens Hammerer,¹ and Anders S. Sørensen³

¹*Institute for Theoretical Physics, Institute for Gravitational Physics (Albert Einstein Institute), Leibniz University Hannover, Appelstraße 2, 30167 Hannover, Germany*

²*Niels Bohr Institute, University of Copenhagen, Blegdamsvej 17, DK-2100 Copenhagen, Denmark*

³*Center for Hybrid Quantum Networks (Hy-Q), Niels Bohr Institute, University of Copenhagen, Blegdamsvej 17, DK-2100 Copenhagen, Denmark*

(Dated: December 3, 2024)

We show that strongly correlated photon transport can be observed in waveguides containing optically dense ensembles of chirally coupled emitters. Remarkably, this occurs for any coupling efficiency $\beta < 1$. Specifically, we compute the photon transport properties through a chirally coupled system of N two-level systems driven by a weak coherent field, where each emitter can also scatter photons out of the waveguide. The photon correlations are due to an interplay of nonlinearity and coupling to a loss reservoir, which creates an effective interaction between transmitted photons. The highly correlated photon states are less susceptible to losses than uncorrelated photons and have a power-law decay with N . This is described using a simple universal asymptotic solution governed by a single scaling parameter which describes the photon bunching and power transmission. We show numerically that, for randomly placed emitters, these results hold even in systems without perfect chirality. The proposal can be implemented in existing tapered fiber setups with trapped atoms.

One of the great challenges of modern optics is to generate strong optical nonlinearities, where individual photons interact with each other [1]. This is encouraged by the wide range of applications enabled by such nonlinearities, including quantum gates on photonic qubits [2] and single photon transistors [3]. Within the realm of quantum optics, the challenge has been taken on with a number of approaches to mediate nonlinear photon-photon interactions, for example, by using single atoms [4–6], gasses of strongly interacting Rydberg atoms [7–9], and artificial quantum emitters such as quantum dots and diamond vacancy centers [10–12]. Experimentally, the key signature of strong quantum nonlinear interactions is the ability to generate strongly bunched photon states from classical driving fields [4, 8, 11, 12]. This has typically been achieved by exploiting a single quantum emitter in a waveguide or cavity as a photon nonlinearity [4, 5, 11]. Therefore, significant effort has been put into increasing the photon-emitter coupling efficiency by embedding single quantum emitters in photonic nanostructures [4, 5, 10, 13]. In addition, photonic nanostructures may be applied to qualitatively change the nature of the light-matter interaction. A recent example is the demonstration of chiral light-matter coupling in photonic fibers and waveguides [14–19], where light emission and propagation may be made directional. Chiral coupling has been implemented to achieve non-reciprocal photon transport [20], may enable the formation of dissipatively driven entangled states [21–23], and can serve as an ingredient for scalable integrated quantum networks [24].

Here we show that chiral coupling in a chain of emitters enables the generation of strong optical nonlinearities sig-

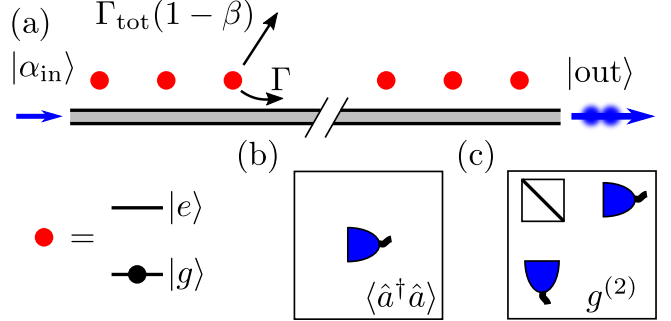


FIG. 1. (a) N chirally coupled two-level emitters (red circles) driven by an external coherent field $|\alpha_{in}\rangle$ with a corresponding strongly correlated output photon state $|\text{out}\rangle$. Each emitter is coupled to the waveguide with a decay rate $\Gamma = \beta\Gamma_{\text{tot}}$ and to external loss modes with a decay rate $\Gamma_{\text{tot}}(1 - \beta)$. The output state is probed by measuring (b) power $\langle \hat{a}^\dagger \hat{a} \rangle$ or (c) the normalized second-order correlation function $g^{(2)}$.

nified by strongly bunched photon transport, even in the case where the single photon-emitter coupling is arbitrarily weak. This constitutes a novel case of strong photon-photon interaction that can be readily observable in experiments on atoms coupled to nanofibers. We present an analytic description of the dynamics of the system of N chirally coupled two-level emitters continuously driven by a weak coherent field while dissipatively coupled to a loss reservoir (Fig. 1(a)). The emitters are coupled to the waveguide with a decay rate $\Gamma = \beta\Gamma_{\text{tot}}$ and radiate to the reservoir with the decay rate $\Gamma_{\text{tot}}(1 - \beta)$, where Γ_{tot} is the total decay rate of the emitters. We determine the photonic output state after interaction with the emitters, and

extract the scaling of the output power and the photon correlations (Fig. 1(b)-(c)) with the number of emitters N . Regardless of the strength of the coupling (i.e. for any $\beta < 1$), we find that the transmission of photons for large N is determined by events where two simultaneously incident photons interact and form a strongly correlated state. As a result, the transmission exhibits a universal power-law decay with N , which means that the photon transport is less susceptible to loss, thereby overcoming the usual exponential decay found for uncorrelated photons. Such long-lived photon pairs are a consequence of an intricate interplay between nonlinear photon interaction and loss. We derive these results analytically assuming chiral interactions, but we show numerically that these conclusions are robust and also apply to bidirectional interactions, i.e. non chiral, for weakly coupled randomly placed emitters.

Solving for the dynamics of N identical chirally coupled quantum emitters can be approached in a variety of ways: it constitutes a cascaded quantum system [25, 26] for which a master equation can be derived [19, 23, 26], but it is challenging to obtain general solutions as the number of emitters increases. Other approaches use a Green function to treat photon propagation and focus on computing the emitter dynamics, but generally require numerical solutions [27, 28]. Here we develop an approach based on scattering matrices. We assume that the emitters are driven at a level well below saturation such that the dynamics of the system can be described by the one- and two-photon Fock states, and thus compute the N -emitter scattering matrix for these manifolds. Computing the single-photon transmission is straightforward [29]. Significant research effort has been put in developing two-photon scattering matrices for a single emitter [30–35], and generalizations to N -emitters have also been developed in the absence of losses [36, 37]. Here we compute the N -emitter two-photon scattering matrix by projecting the input two-photon state on the scattering eigenstates, which can be determined using the Bethe ansatz technique as described in Ref. [32]. Computing the N -emitter scattering matrix simply requires raising the eigenvalues to the N -th power.

The single frequency input coherent state is expressed up to the two-photon state as $|\alpha_{\text{in}}\rangle = e^{-\frac{|\alpha|^2}{2}} \left[1 + \alpha \hat{a}_{k_0}^\dagger + \frac{\alpha^2}{2} \hat{a}_{k_0}^\dagger \hat{a}_{k_0}^\dagger \right] |0\rangle$. We linearize and rescale the waveguide dispersion and set the group velocity $v_g = 1$, such that wavenumber and frequency, as well as distance and time, have the same units. Resonant photons correspond to $k_0 = 0$ and $\hat{a}_{k_0}^\dagger$ creates a photon with detuning k_0 . Unlike bidirectional systems [38], in a chiral system the propagation phase between the emitters amounts to an overall phase in the Markovian limit and does not affect the dynamics [19, 26]. By setting this phase to zero, the N -emitter scattering matrix for up to two photons is $\hat{S}^N = [\hat{S}_{11} + \hat{S}_{22} + \hat{S}_{12}]^N$.

Here, \hat{S}_{11} and \hat{S}_{22} are the one- and two-photon scattering matrices, and \hat{S}_{12} is for two input photons where one is transmitted and the other is lost. This term is required when $\beta < 1$. Note that to ensure that different decays add up incoherently, \hat{S}_{12} contains the state of the photons which are lost. Using the orthogonality of the one- and two-photon subspaces, the scattering matrix restricted to one and two-photons is

$$\hat{S}^N = \hat{S}_{11}^N + \hat{S}_{22}^N + \sum_{M=0}^{N-1} \hat{S}_{11}^{N-M-1} \hat{S}_{12} \hat{S}_{22}^M, \quad (1)$$

and we define contributions to the output state as $\hat{S}^N |\alpha_{\text{in}}\rangle \equiv |\text{out}\rangle_1 + |\text{out}\rangle_2 + |\text{out}\rangle_{21}$. Here, we only consider the part of the scattering with outgoing photons. Computing $\hat{S}_{11}^N |\alpha_{\text{in}}\rangle$ is simple: since the scattering matrix must conserve the photon energy, it simply multiplies the creation operator by a transmission coefficient: $a_k^\dagger \rightarrow t_k^N a_k^\dagger$ with $t_k = 1 - 2\beta/(1 - 2ik/\Gamma_{\text{tot}})$ [34]. This is equivalent to scattering off a single-sided cavity. Consequently, the linear contribution to the output power scales exponentially with N , $\langle a^\dagger a \rangle_1 = |\alpha|^2 |t_{k_0}|^{2N}$. Thus the linear single-photon response yields the usual exponential decay with N when $|t_{k_0}| < 1$.

Computing $\hat{S}_{22}^N |\alpha_{\text{in}}\rangle$ is more involved. We do this by projecting the input state on the orthonormal set of two-photon scattering eigenstates computed in [32]. These consist of a set of extended states $|W_{E,\Delta}\rangle$, with position space representation $W_{E,\Delta}(x_c, x) = \sqrt{2} e^{iE x_c} [2\Delta \cos \Delta x - \Gamma \operatorname{sgn}(x) \sin \Delta x] / (2\pi \sqrt{4\Delta^2 + \Gamma^2})$, where for two photon positions x_1 and x_2 , the centre of mass and difference coordinates are $x_c = (x_1 + x_2)/2$, and $x = x_1 - x_2$ [32]. The two indices of W are a two-photon detuning $E = k + p$ and a frequency difference of the two-photons $\Delta = \frac{k-p}{2}$, where k and p are the detunings of the two photons. The remaining eigenstates are a set of bound states $|B_E\rangle$ with $B_E(x_c, x) = \sqrt{\frac{\Gamma}{4\pi}} e^{iE x_c} e^{-\Gamma/2|x|}$, which only vary with the two-photon detuning E .

The two-photon scattering matrix operating on the input state gives [32]

$$\begin{aligned} |\text{out}\rangle_2 &= \frac{1}{2} \int dE d\Delta t_{\frac{E}{2}+\Delta}^N t_{\frac{E}{2}-\Delta}^N |W_{E,\Delta}\rangle \langle W_{E,\Delta} | \alpha_{\text{in}} \rangle \\ &\quad + \int dE \tilde{t}_E^N |B_E\rangle \langle B_E | \alpha_{\text{in}} \rangle \\ &= A \left[\tilde{t}_{2k_0}^N \sqrt{\frac{8\pi}{\Gamma}} |B_{2k_0}\rangle - \int \frac{d\Delta t_{k_0+\Delta}^N t_{k_0-\Delta}^N}{\Delta \sqrt{1 + 4\frac{\Delta^2}{\Gamma^2}}} |W_{2k_0,\Delta}\rangle \right], \end{aligned} \quad (2)$$

where, henceforth, integrals range over \mathbb{R} , L is a quantization length, and $\tilde{t}_E = 1 - 4\beta/(1 + \beta - iE/\Gamma_{\text{tot}})$. Additionally, $A = \alpha^2/L e^{-\frac{|\alpha|^2}{2}} \sim P_{\text{in}}$ where the input power is $P_{\text{in}} = \alpha^2/L$, and we henceforth take α to be real. Using

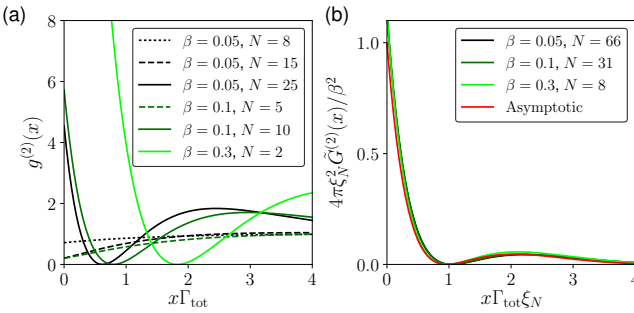


FIG. 2. (a) Normalized second-order correlation function $g^{(2)}(x)$ for different numbers of emitters N and coupling efficiencies β . As the optical depth increases the correlation function becomes strongly bunched. (b) Second-order correlation function $\tilde{G}^{(2)}(x)$ scaled by $4\pi\xi_N^2/\beta^2$. The emitter numbers are chosen so the linear transmission is $(1 - 2\beta)^{2N} \sim 10^{-6}$. In this limit the shape of $\tilde{G}^{(2)}(x)$ is a universal function with scaling parameter ξ_N .

these eigenstates, we obtain a position representation of the full two-photon output state by performing the integral over Δ in (2). The full two-photon output state can be written as

$$|\text{out}\rangle_2 = \frac{A}{2} \int dx_1 dx_2 \hat{a}^\dagger(x_1) \hat{a}^\dagger(x_2) |0\rangle \psi_N(x_c, x), \quad (3)$$

with $\psi_N(x_c, x) = e^{2ik_0x_c} [t_{k_0}^{2N} - \phi_N(x)]$. The $t_{k_0}^{2N}$ term corresponds to uncorrelated photons interacting individually with all N emitters while $\phi_N(x)$ contains the photon correlations induced by the interactions. We calculate the correlations $\phi_N(x)$ analytically, but for brevity, we leave the exact form to the Supplementary Material (SM) and show its asymptotic form below. The correlations induced by the photon-photon interactions are quantified by the normalized second-order correlations function $g^{(2)}(x) = \langle \hat{a}^\dagger(0) \hat{a}^\dagger(x) \hat{a}(x) \hat{a}(0) \rangle / \langle \hat{a}^\dagger \hat{a} \rangle = |\psi_N(x_c, x)|^2 / |t_{k_0}|^{4N} + O(P_{\text{sat}})$, where the saturation power is $P_{\text{sat}} = \Gamma_{\text{tot}}/\beta$. Throughout the remainder of this manuscript we consider a resonant drive $k_0 = 0$ as it generates the most interesting physics.

Figure 2(a) shows $g^{(2)}(x)$ for different β and N . As N increases, $g^{(2)}(x)$ becomes strongly bunched even for $\beta \ll 1$. This signifies that the output contains strong photon-photon correlations and happens because the linear component of the transmitted power $\sim |t_{k_0}|^{2N}$ decays exponentially with N while $\phi_N(x)$ does not. We can understand this by considering the Fourier transform of the correlated part of the two-photon wavepacket $\phi_N(\Delta_k)$, where $\Delta_k = (k_1 - k_2)/2$, which we show in Fig. 3(a). As the two-photon state interacts with emitters the non-linearity of the system generates new frequencies with $\Delta_k \neq 0$, meanwhile the losses of the system are strongest on resonance and thus frequency components $\Delta_k \sim 0$ suffer strong losses. After a sufficient number of scattering events this leads to a two-lobed shape in Fourier space

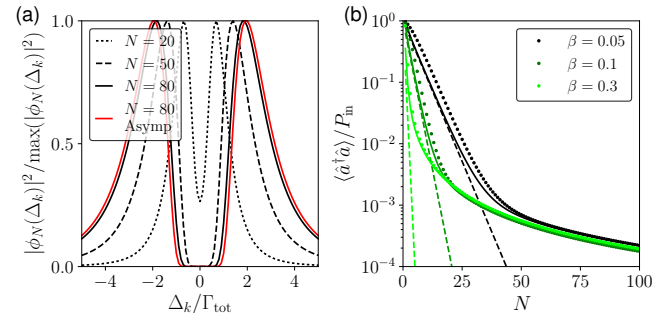


FIG. 3. (a) The normalized magnitude squared of the Fourier Transform of the correlated part of the two-photon wavepacket ϕ_N for $\beta = 0.05$ with the asymptotic expression plotted for $N = 80$ in red. (b) Normalized output intensity $\langle \hat{a}^\dagger \hat{a} \rangle / P_{\text{in}}$ versus emitter number N . Broken lines show the linear output intensity $(1 - 2\beta)^{2N}$ for uncorrelated photon transport while the solid lines show the asymptotic scaling. For large optical depths the transmitted power shows a power-law decay $N^{-3/2}$ and is dominated by correlated photons. The input power is $P_{\text{in}} = 0.1P_{\text{sat}}$.

whose inverse Fourier transform determines the shape of $g^{(2)}(x)$. Since the width of $\phi_N(\Delta_k)$ increases with N , the loss due to each subsequent emitter decreases and thus the scaling of ϕ_N is sub-exponential. We highlight that this behaviour is universal for all $\beta < 1$ provided the optical depth is large. The slow decay of ϕ_N and the resulting large values $g^{(2)}(0)$ reveal that the transmission of the system is dominated by events where two simultaneously incident photons form a correlated state. For sufficiently large optical depth, photons interacting individually will be completely blocked and the transmission is therefore dominated by two-photon events leading to strong photon bunching.

We now derive an asymptotic expression for the non-exponentially decaying parts of ϕ_N . Since detuned Fourier components dominate, we expand the second term in (2) to second order in $\Gamma_{\text{tot}}/\Delta$ and get $t_{\Delta}^N t_{-\Delta}^N \sim \exp[-\Gamma_{\text{tot}}^2 \xi_N^2 / \Delta^2]$, where $\xi_N = \sqrt{N\beta(1-\beta)}$. This gives us a compact expression for the output state in Fourier space (see SM)

$$|\text{out}\rangle_2 \sim -\frac{A\Gamma}{2} \int dk \hat{a}^\dagger(k) \hat{a}^\dagger(-k) |0\rangle \frac{e^{-\xi_N^2 \Gamma_{\text{tot}}^2 / k^2}}{k^2}. \quad (4)$$

The detuned Fourier components thus dominate when $\xi_N^2 \gg 1$. The functional form of this result determines the shape of the curves in Fig. 3(a) and its inverse Fourier Transform gives the shape of $g^{(2)}(x)$ shown in Fig. 2(b). Importantly, it also reveals that the dynamics of two-photon transport is governed universally by ξ_N . This is closely related to the optical depth for a resonant drive which is $\log[(1 - 2\beta)^{2N}] \sim 4\xi_N^2$ when $\beta \sim 0$ or $\beta \sim 1$. We highlight this in Fig. 2(b) which shows the correlation function $\tilde{G}^{(2)}(x) = \langle \hat{a}^\dagger(0) \hat{a}^\dagger(x) \hat{a}(x) \hat{a}(0) \rangle / P_{\text{in}}^2$. Here we multiply the y -axis by $4\pi\xi_N^2/\beta^2$, and the x axis by ξ_N .

The correlation function $\tilde{G}^{(2)}(x)$ then has the same form for all values of β and N as long as the optical depth is large. The rate of transmitted coincident photons $\tilde{G}^{(2)}(0)$ scales as $1/N$ and the width of $\tilde{G}^{(2)}(x)$ scales as $1/\sqrt{N}$. The correlations arising from the complex interplay between nonlinear photon interactions and dissipation can therefore be expressed in a compact form with a simple scaling parameter.

We now turn to the output power. This requires us to compute the contribution due to the last term in (1). Here we construct \hat{S}_{12} by transforming from our picture of a chiral scattering process to one that contains transmission and reflection, where the coupling to the backward mode is given by our decay rate to the loss reservoir $\Gamma_{\text{tot}}(1 - \beta)$. In this picture we simply compute the scattering amplitude for one photon transmitted and one reflected. This is done by adapting standard two-photon scattering matrices for a single emitter (see SM) [34]. We do this independently for each emitter such that there are no collective effects through the loss reservoir, which is a good approximation for non-subwavelength emitter separations [39]. Using this scattering matrix we obtain a state which can be compactly written as

$$|\text{out}\rangle_{21} = \frac{A}{2} \sum_{M=0}^{N-1} \int dk \hat{a}_R^\dagger(k) \hat{a}_L^{\dagger(M+1)}(k) |0\rangle t_k^{N-M-1} b_M(k), \quad (5)$$

where $\hat{a}_R^\dagger(k)$ and $\hat{a}_L^{\dagger(M+1)}(k)$ create right and left going photons and the superscript $M + 1$ ensures there are no collective effects. The function $b_M(k)$ depends on ψ_M and for brevity we leave its exact form for the SM. Importantly, with the state $|\text{out}\rangle_{21}$ at hand we can compute the power $\langle \hat{a}^\dagger \hat{a} \rangle$. Using our exact expressions for $\psi_N(x_c, x)$ and $b_M(k)$ we obtain an expression for $\langle \hat{a}^\dagger \hat{a} \rangle$ containing integrals which we evaluate numerically. These results are shown in Fig. 3(b) for different β and N . Here, uncorrelated photon transport suffers exponential decay with N . Interestingly, we observe that the transmitted power deviates from exponential decay and for large N follows a power law. The nonlinear power transmission therefore dominates for large optical depths.

We use (4) and (5) to compute a simple asymptotic expression for the transmitted power (see SM for details)

$$\frac{\langle \hat{a}^\dagger \hat{a} \rangle}{P_{\text{in}}} \sim (1 - 2\beta)^{2N} + \frac{P_{\text{in}}}{P_{\text{sat}}} \frac{\beta}{4\sqrt{\pi}\xi_N^3} \frac{3 - 2\beta(1 - \beta)}{1 - 2\beta(1 - \beta)}, \quad (6)$$

implying a nonlinear power scaling of $1/N^{3/2}$. Figure 3(b) shows excellent agreement between the full calculation and the asymptotic scaling. We note that $g^{(2)}(x)$ computed to zeroth order from (4) is only valid when the linear transmission is much larger than the nonlinear term which depends on N , β , and $P_{\text{in}}/P_{\text{sat}}$. Finally we note that the nonlinear power has contributions from \hat{S}_{22} and \hat{S}_{12} , i.e., photon pairs and single photons, the nonlinear power contribution of pairs relative to single photons

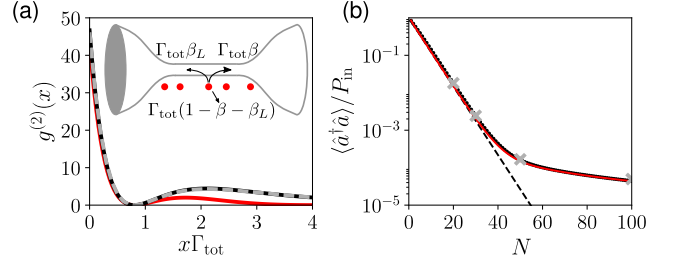


FIG. 4. (a) Normalized second order correlation function for $\beta = 0.05$ and $N = 30$ with inset showing schematic of atoms trapped around a fiber including forward and backward coupling. Solid lines show exact analytic theory (black) and asymptotic theory (red). The broken grey line shows the mean of the numerical simulation averaged over 100 realizations with the inclusion of coupling to the backward propagating mode with $\beta_L = \beta/10$. (b) Normalized output power vs emitter number for $\beta = 0.05$ and $P_{\text{in}}/P_{\text{sat}} = 0.02$ showing the analytic theory (black dots), asymptotic theory (red line), and exponential damping (broken black line). Grey crosses show the mean of the numerical results with $\beta_L = \beta/10$.

is $\langle \hat{a}^\dagger \hat{a} \rangle_2 / \langle \hat{a}^\dagger \hat{a} \rangle_{21} \sim 1/(2\sqrt{2} - 1 + 4\sqrt{2}/(1 - 2\beta(1 - \beta)))$ (see SM), which is largest for $\beta \sim 0$ and $\beta \sim 1$ giving ~ 0.13 , and smallest for $\beta = 1/2$ giving ~ 0.08 .

The physics presented here can be observed experimentally by measuring the second order correlation function and the power of the transmitted light. The nonlinear scaling of the output power and strong photon bunching are clear signals of nonlinear dynamics. State-of-the-art experimental systems that exhibit chiral light-matter interaction include quantum dots (QD) and atoms coupled to photonic nanostructures [15, 16, 40]. In quantum dot systems the emission can be close to unidirectional and $\beta \sim 1$ [16, 41], however it is difficult to tune several QDs into resonance. Resonant interaction has thus far been demonstrated with only a single QD [40, 42]. On the other hand, hundreds of atoms can be trapped in the evanescent field of a nanofibre and exhibit chiral light-matter interaction [15, 43–46] albeit with $\beta \ll 1$. These have a directionality of $\sim 90\%$ and thus couple residually to the backward propagating mode, which has not been taken into account in the analytics here.

We now numerically model a system with parameters similar to a nanofiber with coupling to the forward propagating mode $\beta = 0.05$ and coupling to the backward mode $\beta_L = 0.005$, where the total emission rate to the waveguide is $\Gamma_{\text{tot}}(\beta + \beta_L)$ (Fig. 4(a) inset). We model this system using a wave function formalism where we restrict to two excitations in the system [47, 48], and consider $N = 20, 30, 50, 100$ emitters. The emitters are positioned randomly such that backscattering does not add up coherently. For each parameter set we consider 100 realizations. Figure 4(a) shows the mean of $g^{(2)}(x)$ for $N = 30$ when considering the ensemble. These results agree quantitatively with the exact unidirectional

theory. The slight discrepancy with the asymptotic theory is because parameters do not fall in this limit since $\xi_N^2 = 1.425$. The effects of backscattering can thus be ignored provided the number of emitters is sufficiently large and the emitters are positioned randomly. Figure 4(b) shows the mean output power which is also in excellent agreement with the unidirectional theory. The variance of the power and $g^{(2)}(x)$ is insignificant on the scale of both plots and is not shown.

In order to observe the bunching computed here one must consider an input power and emitter number such that $g^{(2)}$ is sufficiently bunched and such that our zeroth order expression is valid. The linear contribution to the power should thus be significantly larger than the nonlinear part. On the other hand the output power should be sufficiently large to experimentally measure $g^{(2)}(x)$. We find that for $\beta = 0.05$ and $N = 30$ one ideally expects a value of $g^{(2)}(0) = 47$. If we consider an optical transition with $\Gamma_{\text{tot}} = 2\pi \times 5 \text{ MHz}$ driven with $P_{\text{in}}/P_{\text{sat}} = 0.005$, we compute an output power of $\langle \hat{a}^\dagger \hat{a} \rangle = 6 \text{ kHz}$ with the linear part of the power being 12 times larger than the nonlinear part. We also compute a coincidence rate of 17 Hz, where we define a coincidence as two photons separated by less than $3/\Gamma_{\text{tot}}$. This indicates that the zeroth order approximation for $g^{(2)}$ is valid and that the output is sufficiently bright for detection by single photon detectors.

In conclusion we have analyzed the dynamics of photon–photon interactions mediated by an ensemble of emitters chirally coupled to a waveguide. The system exhibits rich out-of-equilibrium physics due to a combination of highly nonlinear driven systems and dissipation. The emitter-induced photon–photon correlation reveals itself through the formation of bunched states of light and a universal power-law scaling of the transmission for large optical depths. As a consequence, for a sufficiently large optical depth the transmission becomes completely dominated by correlated photons. Remarkably, the formation of the strongly correlated photon states happens even for emitters weakly coupled to a waveguide and can thus be directly observed, e.g., with atoms near optical nanofibers. Our work illustrates that chiral coupling obtainable in photonic nanostructures may lead to unexpected and complex transport properties of photons that may find novel applications for constructing integrated quantum photonic devices.

[1] D. E. Chang, V. Vuletić, and M. D. Lukin, *Nat. Photonics* **8**, 685 (2014).

[2] B. Hacker, S. Welte, G. Rempe, and S. Ritter, *Nature* **536**, 193 (2016).

[3] D. E. Chang, A. S. Sørensen, E. A. Demler, and M. D. Lukin, *Nat. Phys.* **3**, 807 (2007).

[4] A. Goban, C.-L. Hung, S.-P. Yu, J. D. Hood, J. A. Muniz, J. H. Lee, M. J. Martin, A. C. McClung, K. S. Choi, D. E. Chang, O. Painter, and H. J. Kimble, *Nat. Commun.* **5**, 3808 (2014).

[5] T. G. Tiecke, J. D. Thompson, N. P. de Leon, L. R. Liu, V. Vuletić, and M. D. Lukin, *Nature* **508**, 241 (2014).

[6] A. Reiserer, N. Kalb, G. Rempe, and S. Ritter, *Nature* **508**, 237 (2014).

[7] M. F. Maghrebi, M. J. Gullans, P. Bienias, S. Choi, I. Martin, O. Firstenberg, M. D. Lukin, H. P. Büchler, and A. V. Gorshkov, *Phys. Rev. Lett.* **115**, 123601 (2015).

[8] O. Firstenberg, T. Peyronel, Q.-Y. Liang, A. V. Gorshkov, M. D. Lukin, and V. Vuletić, *Nature* **502**, 71 (2013).

[9] S. Das, A. Grankin, I. Iakourov, E. Brion, J. Borregaard, R. Boddada, I. Usmani, A. Ourjoumtsev, P. Grangier, and A. S. Sørensen, *Phys. Rev. A* **93**, 040303 (2016).

[10] P. Lodahl, S. Mahmoodian, and S. Stobbe, *Rev. Mod. Phys.* **87**, 347 (2015).

[11] A. Javadi, I. Söllner, M. Arcari, S. Lindskov Hansen, L. Midolo, S. Mahmoodian, G. Kiršanské, T. Pregnolato, E. H. Lee, J. D. Song, S. Stobbe, and P. Lodahl, *Nat. Commun.* **6**, 8655 (2015).

[12] A. Sipahigil, R. E. Evans, D. D. Sukachev, M. J. Burek, J. Borregaard, M. K. Bhaskar, C. T. Nguyen, J. L. Pacheco, H. A. Atikian, C. Meuwly, R. M. Camacho, F. Jelezko, E. Bielejec, H. Park, M. Lončar, and M. D. Lukin, *Science* **354**, 847 (2016).

[13] M. Arcari, I. Söllner, A. Javadi, S. L. Hansen, S. Mahmoodian, J. Liu, H. Thyrrestrup, E. H. Lee, J. D. Song, S. Stobbe, and P. Lodahl, *Phys. Rev. Lett.* **113**, 093603 (2014).

[14] J. Petersen, J. Volz, and A. Rauschenbeutel, *Science* **346**, 67 (2014).

[15] R. Mitsch, C. Sayrin, B. Albrecht, P. Schneeweiss, and A. Rauschenbeutel, *Nat. Commun.* **5**, 5713 (2014).

[16] I. Söllner, S. Mahmoodian, S. L. Hansen, L. Midolo, G. Kiršanské, T. Pregnolato, H. El-Ella, E. H. Lee, J. D. Song, S. Stobbe, and P. Lodahl, *Nat. Nanotechnol.* **10**, 775 (2015).

[17] A. B. Young, A. C. T. Thijssen, D. M. Beggs, P. Androvitsaneas, L. Kuipers, J. G. Rarity, S. Hughes, and R. Oulton, *Phys. Rev. Lett.* **115**, 153901 (2015).

[18] R. J. Coles, D. M. Price, J. E. Dixon, B. Royall, E. Clarke, P. Kok, M. S. Skolnick, A. M. Fox, and M. N. Makhonin, *Nat. Commun.* **7**, 11183 (2016).

[19] P. Lodahl, S. Mahmoodian, S. Stobbe, A. Rauschenbeutel, P. Schneeweiss, J. Volz, H. Pichler, and P. Zoller, *Nature* **541**, 473 (2017).

[20] M. Scheucher, A. Hilico, E. Will, J. Volz, and A. Rauschenbeutel, *Science* **354**, 1577 (2016).

[21] K. Stannigel, P. Rabl, and P. Zoller, *New J. Phys.* **14**, 063014 (2012).

[22] T. Ramos, H. Pichler, A. J. Daley, and P. Zoller, *Phys. Rev. Lett.* **113**, 237203 (2014).

[23] H. Pichler, T. Ramos, A. J. Daley, and P. Zoller, *Phys. Rev. A* **91**, 042116 (2015).

[24] S. Mahmoodian, P. Lodahl, and A. S. Sørensen, *Phys. Rev. Lett.* **117**, 240501 (2016).

[25] H. J. Carmichael, *Phys. Rev. Lett.* **70**, 2273 (1993).

[26] C. W. Gardiner, *Phys. Rev. Lett.* **70**, 2269 (1993).

[27] A. Asenjo-Garcia, J. D. Hood, D. E. Chang, and H. J. Kimble, *Phys. Rev. A* **95**, 033818 (2017).

[28] M. T. Manzoni, D. E. Chang, and J. S. Douglas,

arXiv:1702.05954 (2017).

[29] J. T. Shen and S. Fan, *Opt. Lett.* **30**, 2001 (2005).

[30] K. Kojima, H. F. Hofmann, S. Takeuchi, and K. Sasaki, *Phys. Rev. A* **68**, 013803 (2003).

[31] H. F. Hofmann, K. Kojima, S. Takeuchi, and K. Sasaki, *Phys. Rev. A* **68**, 043813 (2003).

[32] J.-T. Shen and S. Fan, *Phys. Rev. A* **76**, 062709 (2007).

[33] H. Zheng, D. J. Gauthier, and H. U. Baranger, *Phys. Rev. A* **82**, 063816 (2010).

[34] S. Fan, Sükrü Ekin Kocabas, and J.-T. Shen, *Phys. Rev. A* **82**, 063821 (2010).

[35] T. Shi, D. E. Chang, and J. I. Cirac, *Phys. Rev. A* **92**, 053834 (2015).

[36] M. Pletyukhov and V. Gritsev, *New J. Phys.* **14**, 095028 (2012).

[37] M. Ringel, M. Pletyukhov, and V. Gritsev, *New J. Phys.* **16**, 113030 (2014).

[38] D. E. Chang, L. Jiang, A. V. Gorshkov, and H. J. Kimble, *New J. Phys.* **14**, 063003 (2012).

[39] A. Asenjo-Garcia, M. Moreno-Cardoner, A. Albrecht, H. J. Kimble, and D. E. Chang, *Phys. Rev. X* **7**, 031024 (2017).

[40] A. Javadi, D. Ding, M. H. Appel, S. Mahmoodian, M. C. Löbl, I. Söllner, R. Schott, C. Papon, T. Pregnolato, S. Stobbe, L. Midolo, T. Schröder, A. D. Wieck, A. Ludwig, R. J. Warburton, and P. Lodahl, arXiv:1709.06369 (2017).

[41] S. Mahmoodian, K. Prindal-Nielsen, I. Söllner, S. Stobbe, and P. Lodahl, *Opt. Mater. Express* **7**, 43 (2017).

[42] D. M. Price, D. L. Hurst, C. Bentham, M. N. Makhonin, B. Royall, E. Clarke, P. Kok, L. Wilson, M. Skolnick, and A. Fox, arXiv:1801.09958 (2018).

[43] C. Sayrin, C. Junge, R. Mitsch, B. Albrecht, D. O'Shea, P. Schneeweiss, J. Volz, and A. Rauschenbeutel, *Phys. Rev. X* **5**, 041036 (2015).

[44] H. L. Sørensen, J.-B. Béguin, K. W. Kluge, I. Iakourov, A. S. Sørensen, J. H. Müller, E. S. Polzik, and J. Appel, *Phys. Rev. Lett.* **117**, 133604 (2016).

[45] N. V. Corzo, B. Gouraud, A. Chandra, A. Goban, A. S. Sheremet, D. V. Kupriyanov, and J. Laurat, *Phys. Rev. Lett.* **117**, 133603 (2016).

[46] P. Solano, J. A. Grover, J. E. Hoffman, S. Ravets, F. K. Fatemi, L. A. Orozco, and S. L. Rolston, in *Advances In Atomic, Molecular, and Optical Physics*, Vol. 66 (Elsevier, 2017) pp. 439–505.

[47] M. Čepulkovskis, *Nonlinear photon interactions in waveguides*, Master's thesis, Niels Bohr Institute, University of Copenhagen (2017).

[48] S. Das, In preparation (2018).

Supplementary Material: Chiral waveguide QED: Strongly correlated photon transport with weakly coupled emitters

COMPUTING \hat{S}_{22}

In this section we introduce the scattering matrix \hat{S}_{22} and compute the output state $|\text{out}\rangle_2$. We start from the input state

$$\begin{aligned} |\alpha_{\text{in}}\rangle &= e^{-\frac{|\alpha|^2}{2}} \left[1 + \alpha \hat{a}_{k_0}^\dagger + \frac{\alpha^2}{2} \hat{a}_{k_0}^\dagger \hat{a}_{k_0}^\dagger + \dots \right] |0\rangle \\ &= e^{-\frac{|\alpha|^2}{2}} \left[1 + \sqrt{\frac{2\pi}{L}} \alpha \hat{a}^\dagger(k_0) + \frac{2\pi}{L} \frac{\alpha^2}{2} \hat{a}^\dagger(k_0) \hat{a}^\dagger(k_0) + \dots \right] |0\rangle, \end{aligned} \quad (\text{S1})$$

where L is a quantization length, and in the second line we have switched from single-mode operators to operators $\hat{a}_{k_0}^\dagger \rightarrow \sqrt{\frac{2\pi}{L}} \hat{a}^\dagger(k_0)$ suitable for taking the continuum limit $L \rightarrow \infty$. The two-photon scattering matrix in Ref. [32] can be easily generalized to N chirally coupled emitters giving

$$\hat{S}_{22}^N = \frac{1}{2} \int dE d\Delta t_{\frac{E}{2}+\Delta}^N t_{\frac{E}{2}-\Delta}^N |W_{E,\Delta}\rangle \langle W_{E,\Delta}| + \int dE \tilde{t}_E^N |B_E\rangle \langle B_E|, \quad (\text{S2})$$

where all integrals range from $-\infty$ to ∞ , and the two-photon scattering eigenstates in a position-space representation are

$$\begin{aligned} |W_{E,\Delta}\rangle &= \frac{1}{\sqrt{2}} \int dx_1 dx_2 \hat{a}^\dagger(x_1) \hat{a}^\dagger(x_2) |0\rangle W_{E,\Delta}(x_c, x) \\ |B_E\rangle &= \frac{1}{\sqrt{2}} \int dx_1 dx_2 \hat{a}^\dagger(x_1) \hat{a}^\dagger(x_2) |0\rangle B_E(x_c, x). \end{aligned} \quad (\text{S3})$$

Here,

$$\begin{aligned} W_{E,\Delta}(x_c, x) &= \frac{1}{\sqrt{4\Delta^2 + \Gamma^2}} \frac{\sqrt{2}}{2\pi} e^{iEx_c} [2\Delta \cos(\Delta x) - \Gamma \text{sgn}(x) \sin(\Delta x)], \\ B_E(x_c, x) &= \sqrt{\frac{\Gamma}{4\pi}} e^{iEx_c} e^{-\frac{\Gamma}{2}|x|}, \end{aligned} \quad (\text{S4})$$

and

$$\begin{aligned} t_k &= \frac{k + i\Gamma(1 - 2\beta)/(2\beta)}{k + i\Gamma/(2\beta)} \\ \tilde{t}_E &= \frac{E + i\Gamma(1 - 3\beta)/\beta}{E + i\Gamma(1 + \beta)/\beta}, \end{aligned} \quad (\text{S5})$$

and $x_c = \frac{x_1 + x_2}{2}$, $x = x_1 - x_2$, $E = k + p$ is a two-photon detuning, and $\Delta = \frac{k-p}{2}$ is a difference in photon energies, where k and p are photon detunings. The eigenstates $|W_{E,\Delta}\rangle$ and $|B_E\rangle$ form an orthonormal basis for the two-photon subspace [32]. Projecting the input state on the two-photon scattering matrix $|\text{out}\rangle_2 \equiv \hat{S}_{22}^N |\alpha_{\text{in}}\rangle$ gives

$$\begin{aligned} |\text{out}\rangle_2 &= \frac{A}{2} \int dx_1 dx_2 \hat{a}^\dagger(x_1) \hat{a}^\dagger(x_2) |0\rangle \psi_N(x_c, x), \\ \psi_N(x_c, x) &= 2 \tilde{t}_{2k_0}^N e^{2ik_0 x_c} e^{-\frac{\Gamma}{2}|x|} - \frac{\Gamma}{\pi} e^{2ik_0 x_c} \int d\Delta \frac{t_{k_0+\Delta}^N t_{k_0-\Delta}^N}{\Gamma^2 + 4\Delta^2} \left[2 \cos(\Delta x) - \frac{\Gamma}{\Delta} \text{sgn}(x) \sin(\Delta x) \right]. \end{aligned} \quad (\text{S6})$$

These integrals can be computed analytically. For details see the section below. Combining the terms together we obtain

$$\begin{aligned} \psi_N(x_c, x) = e^{2ik_0 x_c} & \left\{ t_{k_0}^{2N} - \frac{i\Gamma/2}{(N-1)!} \frac{d^{N-1}}{dz^{N-1}} \left[\frac{t_{k_0+z}^N (z - k_0 - i\Gamma(1-2\beta)/2\beta)^N e^{iz|x|}}{z^2 + \Gamma^2/4} \right]_{z=k_0 + \frac{i\Gamma}{2\beta}} \right. \\ & + \frac{i\Gamma/2}{(N-1)!} \frac{d^{N-1}}{dz^{N-1}} \left[\frac{t_{k_0-z}^N (z + k_0 + i\Gamma(1-2\beta)/2\beta)^N e^{-iz|x|}}{z^2 + \Gamma^2/4} \right]_{z=-k_0 - \frac{i\Gamma}{2\beta}} \\ & + \frac{\Gamma^2/4}{(N-1)!} \frac{d^{N-1}}{dz^{N-1}} \left[\frac{t_{k_0+z}^N (z - k_0 - i\Gamma(1-2\beta)/2\beta)^N e^{iz|x|}}{z(z^2 + \Gamma^2/4)} \right]_{z=k_0 + \frac{i\Gamma}{2\beta}} \\ & \left. + \frac{\Gamma^2/4}{(N-1)!} \frac{d^{N-1}}{dz^{N-1}} \left[\frac{t_{k_0-z}^N (z + k_0 + i\Gamma(1-2\beta)/2\beta)^N e^{-iz|x|}}{z(z^2 + \Gamma^2/4)} \right]_{z=-k_0 - \frac{i\Gamma}{2\beta}} \right\}, \end{aligned} \quad (S7)$$

which expresses the solution in terms of an $(N-1)$ th order differential operator. These differential operators can be evaluated in terms of generalized functions (see section below). Using the results leading up to (S65) we express the two-photon wavefunction as

$$\psi_N(x_c, x) = e^{2ik_0 x_c} \left\{ t_{k_0}^{2N} - \frac{1}{(N-1)!} \sum_{n=0}^{N-1} \binom{N-1}{n} F_{k_0}(N, n) \chi_{k_0, N-1-n}(x) \right\}, \quad (S8)$$

where $F_{k_0}(N, n)$ is given by (S52) and $\chi_{k_0, n}(x)$ by (S66). This is defined in the main text as $\psi_N(x_c, x) = e^{2ik_0 x_c} [t_{k_0}^{2N} - \phi_N(x)]$.

It is also useful to express the two-photon output state in k -space. We simply rewrite (S6) in terms of creation operators $\hat{a}^\dagger(k_1)$ and $\hat{a}^\dagger(k_2)$

$$|\text{out}\rangle_2 = \frac{A}{2} \int dk_1 dk_2 \hat{a}^\dagger(k_1) \hat{a}^\dagger(k_2) |0\rangle \psi_N(E_k, \Delta_k), \quad (S9)$$

where $E_k = k_1 + k_2$ and $\Delta_k = (k_1 - k_2)/2$ and

$$\psi_N(E_k, \Delta_k) = \delta(E_k - 2k_0) \left\{ 2\pi\delta(\Delta_k) t_{k_0}^{2N} - \frac{1}{(N-1)!} \sum_{n=0}^{N-1} \binom{N-1}{n} F_{k_0}(N, n) \chi_{N-1-n, k_0}(\Delta_k) \right\}. \quad (S10)$$

We have

$$\chi_{n, k_0}(\Delta_k) = n! \Gamma \left\{ \frac{[-\Delta_k - \gamma]^{-n-1}}{\Delta_k(\Delta_k + \frac{i\Gamma}{2})} + \frac{[\Delta_k - \gamma]^{-n-1}}{\Delta_k(\Delta_k - \frac{i\Gamma}{2})} - \frac{2}{\Delta_k^2 + \frac{\Gamma^2}{4}} \left(\frac{-1}{a} \right)^{n+1} \right\}, \quad (S11)$$

$\gamma = k_0 + i\Gamma/2\beta$, and $a = k_0 + i\Gamma(1-2\beta)/2\beta$. We define in a compact form $\psi_N(E_k, \Delta_k) = \delta(E_k - 2k_0) [2\pi\delta(\Delta_k) t_{2k_0}^{2N} - \phi_N(\Delta_k)]$.

CONSTRUCTING AND COMPUTING \hat{S}_{12}

In this section we compute the term due to one photon being scattered out of the waveguide and the other being transmitted. Each of the N emitters contributes to this term and we therefore have to sum over all the emitters. We start by applying the scattering matrix in Eq. (1) on the input state and obtain the k -space result for the two-photon output state after scattering off M emitters,

$$2\pi \frac{A}{2} \sum_{M=0}^{N-1} \hat{S}_{11}^{N-M-1} \hat{S}_{12} \hat{S}_{22}^M \hat{a}^\dagger(k_0) \hat{a}^\dagger(k_0) |0\rangle = \frac{A}{2} \sum_{M=0}^{N-1} \hat{S}_{11}^{N-M-1} \hat{S}_{12} \int dk_1 dk_2 \psi_M(E_k, \Delta_k) \hat{a}^\dagger(k_1) \hat{a}^\dagger(k_2) |0\rangle. \quad (S12)$$

The task at hand is thus to apply \hat{S}_{12} to each term in the sum.

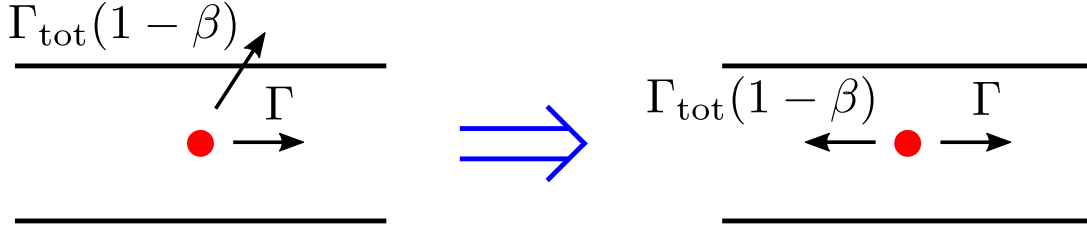


FIG. S1. For a single emitter we can map a unidirectional system with losses to a bidirectional system. We can use this to compute the multi-emitter scattering matrix \hat{S}_{12} by ignoring collective effects.

We construct \hat{S}_{12} by mapping a chiral interaction with losses to a bidirectional waveguide where the emission rate to the backward propagating mode is the same as the loss rate in the chiral system as illustrated in Fig. S1. From this we can construct \hat{S}_{12} from the scattering matrix for one photon transmitted and one reflected by adapting the process outlined in Ref. [34]. This scattering matrix for an arbitrary two-photon wavefunction $f(k_1, k_2)$ is

$$\begin{aligned} \hat{S}_{12} \int dk_1 dk_2 \hat{a}^\dagger(k_1) \hat{a}^\dagger(k_2) |0\rangle f(k_1, k_2) = & \int dk_1 dk_2 \hat{a}_R^\dagger(k_1) \hat{a}_L^\dagger(-k_2) |0\rangle \left[2\bar{r}_{-k_2} t_{k_1} f(k_1, -k_2) \right. \\ & \left. + \frac{i\beta\sqrt{\Gamma(1-\beta)}}{\pi} \bar{s}_{k_1} \bar{s}_{-k_2} \int dp_1 dp_2 (\bar{s}_{p_1} + \bar{s}_{p_2}) \delta(k_1 - k_2 - p_1 - p_2) f(p_1, p_2) \right], \end{aligned} \quad (\text{S13})$$

where \hat{a}_R^\dagger creates a forward-propagating photon and \hat{a}_L^\dagger creates a backward propagating photon, and backwards photons have negative wavevectors. Here, $\bar{r}_k = -2i\sqrt{\beta(1-\beta)}/(1-2ik/\Gamma_{\text{tot}})$ and $\bar{s}_k = \sqrt{\Gamma_{\text{tot}}}/(k+i\Gamma_{\text{tot}}/2)$, where we have used the overbar as these definitions differ from those typically used in the literature. Applying \hat{S}_{12} and S_{11} in (S12) gives

$$\begin{aligned} |\text{out}\rangle_{21} = & \frac{A}{2} \sum_{M=0}^{N-1} \int dk_1 dk_2 t_{k_1}^{N-M-1} \hat{a}_R^\dagger(k_1) \hat{a}_L^{\dagger(M+1)}(-k_2) |0\rangle \left[2\bar{r}_{-k_2} t_{k_1} \psi_M \left(2\Delta_k, \frac{E_k}{2} \right) + \frac{i\beta\sqrt{\Gamma(1-\beta)}}{\pi} \right. \\ & \left. \times \bar{s}_{k_1} \bar{s}_{-k_2} \int dE_p d\Delta_p \left(\bar{s}_{\frac{E_p}{2} + \Delta_p} + \bar{s}_{\frac{E_p}{2} - \Delta_p} \right) \delta(2\Delta_k - E_p) \psi_M(E_p, \Delta_p) \right], \end{aligned} \quad (\text{S14})$$

where the superscript $(M+1)$ on \hat{a}^\dagger ensures each emitter is coupled to a separate reservoir such that the loss reservoir does not mediate collective effects. Considering a resonant drive $k_0 \rightarrow 0$ and using the expression for $\psi_N(E_k, \Delta_k)$ in (S9) after some manipulation we obtain

$$\begin{aligned} |\text{out}\rangle_{21} = & \frac{A}{2} \sum_{M=0}^{N-1} \int dk t_k^{N-M-1} \hat{a}_R^\dagger(k) \hat{a}_L^{\dagger(M+1)}(-k) |0\rangle \left\{ 4\pi \bar{r}_{-k} t_k t_0^{2M} \delta(k) - 2\bar{r}_{-k} t_k \phi_M(k) \right. \\ & \left. + \frac{i\beta\sqrt{\Gamma(1-\beta)}}{\pi} \bar{s}_k \bar{s}_{-k} [4\pi \bar{s}_0 t_0^{2M} - \Phi_M] \right\} \\ \equiv & \frac{A}{2} \sum_{M=0}^{N-1} \int dk t_k^{N-M-1} \hat{a}_R^\dagger(k) \hat{a}_L^{\dagger(M+1)}(-k) |0\rangle b_M(k), \end{aligned} \quad (\text{S15})$$

which gives (5) in the main text. Here, we also define

$$c_M(k) = \left\{ -2\bar{r}_{-k} t_k \phi_M(k) + \frac{i\beta\sqrt{\Gamma(1-\beta)}}{\pi} \bar{s}_k \bar{s}_{-k} [4\pi \bar{s}_0 t_0^{2M} - \Phi_M] \right\}, \quad (\text{S16})$$

which is the correlated part of $|\text{out}\rangle_{21}$. The term $\Phi_M = \int dk (\bar{s}_k + \bar{s}_{-k}) \phi_M(k)$ can be computed analytically (see section below).

OUTPUT POWER

In this section we compute the power output after N emitters for a resonant drive. The terms $|\text{out}\rangle_1$, $|\text{out}\rangle_2$, and $|\text{out}\rangle_{21}$ all contribute to this, and we write $\langle \hat{a}^\dagger \hat{a} \rangle = \langle \hat{a}^\dagger \hat{a} \rangle_1 + \langle \hat{a}^\dagger \hat{a} \rangle_2 + \langle \hat{a}^\dagger \hat{a} \rangle_{21}$. We note that the system is at steady state so we evaluate the power at $x = 0$ without loss of generality. Computing $\langle \hat{a}^\dagger \hat{a} \rangle_1$ is straightforward and gives $\langle \hat{a}^\dagger \hat{a} \rangle_1 = \frac{|\alpha|^2 e^{-|\alpha|^2}}{L} t_0^{2N} \sim t_0^{2N} (|\alpha|^2/L - |\alpha|^4 L/L^2)$, where $t_0 = 1 - 2\beta$. The term $|\alpha|^4 L/L^2$ is non-physical as it scales with L (after taking into account that the input power is $P_{\text{in}} = |\alpha|^2/L$). We below show that it cancels with similar unphysical terms from the two-photon contribution.

Moving to $\langle \hat{a}^\dagger \hat{a} \rangle_2$, we compute $\hat{a}(x=0)|\text{out}\rangle_2$ and use this to find

$$\langle \hat{a}^\dagger \hat{a} \rangle_2 = \frac{e^{-|\alpha|^2} |\alpha|^4}{L^2} \left[|t_0|^{4N} L + \int dx |\phi_N(x)|^2 - 2 t_0^{2N} \int dx \phi_N(x) \right]. \quad (\text{S17})$$

Again, the first term here is non-physical as it depends on L . This term cancels with the similar non-physical term from $\langle \hat{a}^\dagger \hat{a} \rangle_{21}$. Using (S14) we compute $\langle \hat{a}^\dagger \hat{a} \rangle_{21}$

$$\langle \hat{a}^\dagger \hat{a} \rangle_{21} = \frac{e^{-|\alpha|^2} |\alpha|^4}{L^2} \sum_{M=0}^{N-1} \left\{ \bar{r}_0^2 t_0^{2(N+M)} L + \frac{1}{8\pi} \int dk |c_M(k)|^2 + \text{Re} [\bar{r}_0 t_0^{N+M} c_M(0)] \right\}, \quad (\text{S18})$$

where we note that t_0 and \bar{r}_0 are real-valued on resonance. Combining these together to fourth order in $|\alpha|$ gives

$$\langle \hat{a}^\dagger \hat{a} \rangle = \frac{|\alpha|^2}{L} |t_0|^{2N} + \frac{|\alpha|^4}{L^2} \left\{ \int dx |\phi_N(x)|^2 - 2 t_0^{2N} \int dx \phi_N(x) + \sum_{M=0}^{N-1} \frac{1}{8\pi} \int dk |c_M(k)|^2 + \text{Re} [r_0 t_0^{N+M} c_M(0)] \right\}, \quad (\text{S19})$$

where we have used $t_0^{4N} - t_0^{2N} + \sum_{M=0}^{N-1} \bar{r}_0^2 t_0^{2(N+M)} = 0$ and thus all the non-physical terms vanish. We note that the input power is $P_{\text{in}} = |\alpha|^2/L$ and has units of photons per length. Since we have set $v_g = 1$ throughout it also has units of photons per time. We perform the integrals in (S19) numerically to produce the plot in Fig. 3(b).

ASYMPTOTICS

Here we compute the correlation function and the output power in the limit of the dynamics being dominated by detuned Fourier components. From Fig. 3(a) of the main text we have observed that when the optical depth becomes large the Fourier spectrum of the two-photon wavefunction is dominated by detuned Fourier components. By expanding to second order in Γ/Δ we obtain asymptotic expressions for $|\text{out}\rangle_2$, $|\text{out}\rangle_{21}$ and $\langle \hat{a}^\dagger \hat{a} \rangle$. Starting from Eq. (3), we assume a resonant drive and ignore terms that decrease exponentially in N and thus write

$$|\text{out}\rangle_2 \sim -A \int \frac{d\Delta t_\Delta^N t_{-\Delta}^N}{\Delta \sqrt{1 + 4\frac{\Delta^2}{\Gamma^2}}} \left\{ \frac{1}{\sqrt{2}} \int dx_1 dx_2 \hat{a}^\dagger(x_1) \hat{a}^\dagger(x_2) |0\rangle \frac{1}{\sqrt{4\Delta^2 + \Gamma^2}} \frac{\sqrt{2}}{2\pi} [2\Delta \cos(\Delta x) - \Gamma \text{sgn}(x) \sin(\Delta x)] \right\}. \quad (\text{S20})$$

Expanding to second order, we write $t_\Delta^N t_{-\Delta}^N \sim \exp[-\xi_N^2 \frac{\Gamma_{\text{tot}}^2}{\Delta^2}]$, with $\xi_N = \sqrt{N\beta(1-\beta)}$ and thus our assumption of detuned frequencies dominating implies $N\beta(1-\beta) = \xi_N^2 \gg 1$. We thus have

$$|\text{out}\rangle_2 \sim -A \frac{\Gamma}{4\pi} \int dx_1 dx_2 \hat{a}^\dagger(x_1) \hat{a}^\dagger(x_2) |0\rangle \int d\Delta \frac{e^{-\xi_N^2 \Gamma_{\text{tot}}^2 / \Delta^2}}{\Delta^2} \cos(\Delta x), \quad (\text{S21})$$

and we define

$$F_N(x) = \int d\Delta \frac{e^{-\xi_N^2 \Gamma_{\text{tot}}^2 / \Delta^2}}{\Delta^2} \cos(\Delta x) = \frac{\sqrt{\pi}}{\Gamma_{\text{tot}} \xi_N} {}_0F_2 \left(\frac{1}{2}, \frac{1}{2}; \frac{\xi_N^2 \Gamma_{\text{tot}}^2 x^2}{4} \right) - \pi |x| {}_0F_2 \left(1, \frac{3}{2}; \frac{\xi_N^2 \Gamma_{\text{tot}}^2 x^2}{4} \right), \quad (\text{S22})$$

where ${}_0F_2$ is the generalized hypergeometric function. From this we obtain $g^{(2)}(x) \sim \frac{\Gamma^2}{4\pi^2} \frac{|F_N(x)|^2}{(1-2\beta)^{4N}}$. We furthermore obtain a k -space representation of (S21) as

$$|\text{out}\rangle_2 \sim -A \frac{\Gamma}{2} \int dk_1 dk_2 \hat{a}^\dagger(k_1) \hat{a}^\dagger(k_2) |0\rangle \delta(E_k) \frac{e^{-\xi_N^2 \Gamma_{\text{tot}}^2 / \Delta_k^2}}{\Delta_k^2}, \quad (\text{S23})$$

where we define $\phi_N^{\text{asymp}}(\Delta_k) = \Gamma/\Delta_k^2 \exp[-\xi_N^2 \Gamma_{\text{tot}}^2/\Delta_k^2]$. With the two-photon wavefunction at hand we easily obtain the two-photon contribution to the nonlinear part of the power

$$\langle \hat{a}^\dagger \hat{a} \rangle_2 \sim \frac{P_{\text{in}}}{P_{\text{sat}}} \frac{1}{8\sqrt{2\pi}} \frac{\beta}{\xi_N^3}. \quad (\text{S24})$$

We now compute the output power $\langle \hat{a}^\dagger \hat{a} \rangle_{21}$ using (S18) and $\phi_N^{\text{asymp}}(\Delta_k)$. We do this by first obtaining an asymptotic expression for $|\text{out}\rangle_{21}$. We consider terms scaling sub-exponentially in N , and thus drop the terms that are exponential in N . This leaves the contribution which is proportional to $c_M(k)$ (see (S16)). Within the asymptotic limit, the contribution here from Φ_M is smaller than the other terms. This term contains processes where one photon is scattered out of the waveguide while the other is transmitted through a correlated nonlinear process. This is unlikely to occur because the correlated wavefunction $\phi_N^{\text{asymp}}(\Delta_k)$ is dominated by detuned Fourier components and is unlikely to interact nonlinearly. We are thus left with

$$|\text{out}\rangle_{21} = \frac{A}{2} \sum_{M=0}^{N-1} \int dk \hat{a}_R^\dagger(k) \hat{a}_L^{\dagger(M+1)}(-k) |0\rangle t_k^{N-M-1} \left\{ -2\bar{r}_{-k} t_k \phi_M^{\text{asymp}}(k) + \frac{i\beta\sqrt{\Gamma(1-\beta)}}{\pi} \bar{s}_k \bar{s}_{-k} 4\pi \bar{s}_0 t_0^{2M} \right\}. \quad (\text{S25})$$

The first term contains the asymptotic form $\phi_M^{\text{asymp}}(k)$ interacting linearly with emitters and the second term quantifies the correlated interactions, i.e. the two photons interact in an uncorrelated manner for the first M emitters and then interact in a correlated manner on the $M+1$ th emitter through the \hat{S}_{12} scattering term. Computing $\langle \hat{a}^\dagger \hat{a} \rangle_{21}$ leads to three integrals: the modulus square of the first and second terms in (S25) and the cross term. We have found that the cross term does not contribute to leading order and we thus focus on the other two. First, we have

$$\begin{aligned} \int dk |r_{-k}|^2 |t_k|^{2(N-M)} |\phi_M^{\text{asymp}}(k)|^2 &\sim \beta(1-\beta) \Gamma_{\text{tot}}^2 \Gamma^2 \int dk \frac{e^{-\xi_{N+M}^2 \Gamma_{\text{tot}}^2/k^2}}{k^6} \\ &= \frac{\beta^3(1-\beta) 3\sqrt{\pi}}{\xi_{N+M}^5 \Gamma_{\text{tot}}}, \end{aligned} \quad (\text{S26})$$

where we have used $|t_k|^{2N} \sim \exp[-\xi_N^2 \frac{\Gamma_{\text{tot}}^2}{k^2}]$, and the integral $\int dk e^{-c^2/k^2}/k^{2n} = \Gamma(n - \frac{1}{2})/c^{2n-1}$, where $\Gamma(n)$ is the Gamma function. The contribution from the modulus square of the second term in (S25) decays exponentially with M and is thus dominated by terms $M \ll N$. This allows writing to leading order

$$\begin{aligned} \int dk |\bar{s}_k \bar{s}_{-k}|^2 |t_k|^{2(N-M-1)} &\sim \int dk e^{-\xi_{N-M-1}^2 \Gamma_{\text{tot}}^2/k^2} \frac{\Gamma_{\text{tot}}^2}{k^4} \\ &\sim \frac{\sqrt{\pi}}{2 \xi_{N-M}^3 \Gamma_{\text{tot}}}. \end{aligned} \quad (\text{S27})$$

Using these integrals and (S25) we get

$$\begin{aligned} \frac{\langle \hat{a}^\dagger \hat{a} \rangle_{21}}{P_{\text{in}}} &\sim \frac{P_{\text{in}}}{8\pi} \sum_{M=0}^{N-1} \left\{ \frac{\beta^3(1-\beta) 3\sqrt{\pi}}{\xi_{N+M}^5 \Gamma_{\text{tot}}} + 64\beta^3(1-\beta) t_0^{4M} \frac{\sqrt{\pi}}{2 \xi_N^3 \Gamma_{\text{tot}}} \right\} \\ &\sim \frac{P_{\text{in}}}{P_{\text{sat}}} \left[\frac{2\sqrt{2}-1}{8\sqrt{2\pi}} + \frac{1}{2\sqrt{\pi}} \frac{1}{1-2\beta(1-\beta)} \right] \frac{\beta}{\xi_N^3} \end{aligned} \quad (\text{S28})$$

where, for the first term, we have used $\sum_{M=0}^{N-1} 1/(N+M)^{5/2} = \zeta(\frac{5}{2}, N) - \zeta(\frac{5}{2}, 2N) \sim \left(\frac{2}{3} - \frac{1}{3\sqrt{2}}\right) \frac{1}{N^{3/2}}$ for $N \gg 1$, where $\zeta(s, a)$ is the Hurwitz zeta function, and for the second term we extended the summation to ∞ and computed the geometric series. Combining (S24), (S28), and the linear contribution gives Eq. 6 in the main text.

COMPUTING THE INTEGRALS

In this section we compute the values of the integrals used throughout the manuscript. The first integral is

$$I_1 = \int d\Delta \frac{t_{k_0+\Delta}^N t_{k_0-\Delta}^N}{\Gamma^2 + 4\Delta^2} \cos(\Delta x) = \frac{1}{2} \int d\Delta \frac{e^{i\Delta|x|} + e^{-i\Delta|x|}}{\Gamma^2 + 4\Delta^2} \left(\frac{\Delta + k_0 + i\Gamma(1-2\beta)/2\beta}{\Delta + k_0 + i\Gamma/2\beta} \right)^N \left(\frac{\Delta - k_0 - i\Gamma(1-2\beta)/2\beta}{\Delta - k_0 - i\Gamma/2\beta} \right)^N. \quad (\text{S29})$$

By extending the integrand over the entire complex plane and using a contour that is closed in the upper or lower half of the complex plane the above integral can be computed using the Residue Theorem. This gives

$$I_1 = \frac{\pi}{4\Gamma} \left\{ 2\tilde{t}_{2k_0}^N e^{-\frac{\Gamma}{2}|x|} + \frac{i\Gamma}{(N-1)!} \frac{d^{N-1}}{dz^{N-1}} \left[\frac{t_{k_0+z}^N (z - k_0 - i\Gamma(1-2\beta)/2\beta)^N e^{iz|x|}}{z^2 + \Gamma^2/4} \right]_{z=k_0+\frac{i\Gamma}{2\beta}} \right. \\ \left. - \frac{i\Gamma}{(N-1)!} \frac{d^{N-1}}{dz^{N-1}} \left[\frac{t_{k_0-z}^N (z + k_0 + \Gamma(1-2\beta)/2\beta)^N e^{-iz|x|}}{z^2 + \Gamma^2/4} \right]_{z=-k_0-\frac{i\Gamma}{2\beta}} \right\}, \quad (\text{S30})$$

where we have used $t_{k_0+\frac{i\Gamma}{2}} t_{k_0-\frac{i\Gamma}{2}} = \tilde{t}_{2k_0}$.

The second integral we compute is

$$I_2 = \text{sgn}(x) \int \frac{d\Delta}{\Delta} \frac{t_{k_0+\Delta}^N t_{k_0-\Delta}^N}{\Gamma^2 + 4\Delta^2} \sin(\Delta x) = \frac{1}{2i} \int \frac{d\Delta}{\Delta} \frac{e^{i\Delta|x|} - e^{-i\Delta|x|}}{\Gamma^2 + 4\Delta^2} \left(\frac{\Delta + k_0 + i\Gamma(1-2\beta)/2\beta}{\Delta + k_0 + i\Gamma/2\beta} \right)^N \\ \times \left(\frac{\Delta - k_0 - i\Gamma(1-2\beta)/2\beta}{\Delta - k_0 - i\Gamma/2\beta} \right)^N. \quad (\text{S31})$$

Using the same approach as for I_1 we obtain

$$I_2 = \frac{i\pi}{4\Gamma} \left\{ -\frac{4i}{\Gamma} t_{k_0}^{2N} + \frac{4i}{\Gamma} \tilde{t}_{2k_0}^N e^{-\frac{\Gamma}{2}|x|} - \frac{i\Gamma}{(N-1)!} \frac{d^{N-1}}{dz^{N-1}} \left[\frac{t_{k_0+z}^N (z - k_0 - i\Gamma(1-2\beta)/2\beta)^N e^{iz|x|}}{z(z^2 + \Gamma^2/4)} \right]_{z=k_0+\frac{i\Gamma}{2\beta}} \right. \\ \left. - \frac{i\Gamma}{(N-1)!} \frac{d^{N-1}}{dz^{N-1}} \left[\frac{t_{k_0-z}^N (z + k_0 + \Gamma(1-2\beta)/2\beta)^N e^{-iz|x|}}{z(z^2 + \Gamma^2/4)} \right]_{z=-k_0-\frac{i\Gamma}{2\beta}} \right\}. \quad (\text{S32})$$

The third integral, which we compute for a resonant drive, is

$$\Phi_N = \int dk (\bar{s}_k + \bar{s}_{-k}) \phi_M(k) = \frac{1}{(N-1)!} \sum_{j=0}^{N-1} \binom{N-1}{j} F_0(N, j) \int dk (\bar{s}_k + \bar{s}_{-k}) \chi_{N-1-j}(k) \\ = \Gamma \sum_{j=0}^{N-1} \frac{F_0(N, j)}{j!} \int dk (\bar{s}_k + \bar{s}_{-k}) \left[\frac{(k - \frac{i\Gamma}{2\beta})^{j-N}}{k(k - \frac{i\Gamma}{2})} + \frac{(-k - \frac{i\Gamma}{2\beta})^{j-N}}{k(k + \frac{i\Gamma}{2})} - \frac{2}{k^2 + \frac{\Gamma^2}{4}} \left(\frac{2i\beta}{\Gamma(1-\beta)} \right)^{N-j} \right] \quad (\text{S33})$$

The third term in the square brackets is evaluated easily

$$\Phi_N^{(3)} = \int dk (\bar{s}_k + \bar{s}_{-k}) \frac{2\Gamma}{k^2 + \frac{\Gamma^2}{4}} = \frac{-16i\pi\sqrt{\beta/\Gamma}}{1+\beta}. \quad (\text{S34})$$

The first two terms in the square brackets of (S33) can be combined to give an integral of the form

$$\Phi_N^{(1)} + \Phi_N^{(2)} = \int dk \frac{\Gamma(\bar{s}_k + \bar{s}_{-k})}{k(k^2 + \frac{\Gamma^2}{4})(k^2 + \frac{\Gamma^2}{4\beta^2})^{N-j}} \left\{ k \left[\left(k + \frac{i\Gamma}{2\beta} \right)^{N-j} + (-1)^{N-j} \left(k - \frac{i\Gamma}{2\beta} \right)^{N-j} \right] \right. \\ \left. + \frac{i\Gamma}{2} \left[\left(k + \frac{i\Gamma}{2\beta} \right)^{N-j} - (-1)^{N-j} \left(k - \frac{i\Gamma}{2\beta} \right)^{N-j} \right] \right\}. \quad (\text{S35})$$

Using a binomial series to expand the powers in the braces, the entire expression can be written as

$$\Phi_N^{(1)} + \Phi_N^{(2)} = \sum_{m=0}^{N-j} \binom{N-j}{m} \left(\frac{i\Gamma}{2\beta} \right)^{N-j-m} I_{m, N-j}, \quad (\text{S36})$$

where

$$I_{m, N-j} = \begin{cases} \int dk \frac{2\Gamma(\bar{s}_k + \bar{s}_{-k}) k^m}{\left(k^2 + \frac{\Gamma^2}{4} \right) \left(k^2 + \frac{\Gamma^2}{4\beta^2} \right)^{N-j}} & \text{if } m \in \text{even} \\ \int dk \frac{i\Gamma^2 (\bar{s}_k + \bar{s}_{-k}) k^{m-1}}{\left(k^2 + \frac{\Gamma^2}{4} \right) \left(k^2 + \frac{\Gamma^2}{4\beta} \right)^{N-j}} & \text{if } m \in \text{odd}, \end{cases} \quad (\text{S37})$$

which can be evaluated to give

$$I_{k,j} = \begin{cases} 64\pi(-1)^{j+1}i^{k+1}2^{2j-k}\beta^{\frac{3}{2}+2j}\Gamma^{-\frac{5}{2}-2j}\left[\beta(-1+\beta^2)^{-2-j}\Gamma^k - \Gamma_{\text{tot}}^k \frac{\Gamma(\frac{k+1}{2})}{\Gamma(j+2)} {}_2\tilde{F}_1\left(\frac{1}{2}, \frac{1+k}{2}; \frac{1}{\beta^2}; \frac{1}{\beta^2}\right)\right] & \text{if } k \in \text{even} \\ 64\Gamma_{\text{tot}}^{-\frac{5}{2}-2j}2^{2j-k}\left[\Gamma_{\text{tot}}^k \Gamma\left(2+j-\frac{k}{2}\right) \Gamma\left(\frac{k}{2}\right) {}_2F_1\left(\frac{1}{2}, \frac{k}{2}; \frac{1}{\beta^2}; \frac{1}{\beta^2}\right) + (-1)^{\frac{2j+k-1}{2}}\pi(-1+\beta^2)^{-2-j}\Gamma^k\right] & \text{if } k \in \text{odd}, \end{cases} \quad (\text{S38})$$

where ${}_2F_1$ is Gauss's Hypergeometric function and ${}_2\tilde{F}_1$ is Gauss's regularized Hypergeometric function. Putting everything together we get

$$\Phi_N = \sum_{j=0}^{N-1} \frac{F_0(N, j)}{j!} \left[\frac{16i\pi\sqrt{\beta/\Gamma}}{1+\beta} \left(\frac{2i\beta}{\Gamma(1-\beta)} \right)^{N-j} + \sum_{m=0}^{N-j} \binom{N-j}{m} \left(\frac{i\Gamma}{2\beta} \right)^{N-j-m} I_{m, N-j} \right] \quad (\text{S39})$$

COMPUTING THE DIFFERENTIALS

In this section we compute the differentials that emerge from the evaluation of the residue of the N th order poles in integrals I_1 and I_2 . In total there are four differentials in (S7). Here we detail the steps we use to evaluate these in terms of generalized functions.

In this section we make extensive use of the general Leibniz rule of differentiation

$$\frac{d^n}{dx^n} [f(x)g(x)]_{x=x_0} = \sum_{i=0}^n \binom{n}{i} \frac{d^i f(x)}{dx^i} \bigg|_{x=x_0} \frac{d^{n-i} g(x)}{dx^{n-i}} \bigg|_{x=x_0}. \quad (\text{S40})$$

We start with the first differential in (S7) and write it in a compact form

$$\frac{1}{(N-1)!} \frac{d^{N-1}}{dz^{N-1}} \left[t_{k_0+z}^N \left(z - k_0 - \frac{i\Gamma}{2\beta}(1-2\beta) \right)^N \frac{e^{iz|x|}}{z^2 + \Gamma^2/4} \right]_{z=k_0+\frac{i\Gamma}{2\beta}} \equiv \frac{1}{(N-1)!} \frac{d^{N-1}}{dz^{N-1}} \left[[f(z)]^N g(z, x) \right]_{z=\gamma}, \quad (\text{S41})$$

where $\gamma = k_0 + i\Gamma/2\beta$, $f(z) = t_{k_0+z}(z - k_0 - \frac{i\Gamma}{2\beta}(1-2\beta))$, and $g(z, x) = e^{iz|x|}/(z^2 + \Gamma^2/4)$. Using Leibniz's rule this becomes

$$\frac{1}{(N-1)!} \frac{d^{N-1}}{dz^{N-1}} \left[[f(z)]^N g(z, x) \right]_{z=\gamma} = \frac{1}{(N-1)!} \sum_{m=0}^{N-1} \binom{N-1}{m} \frac{d^m [f(z)]^N}{dz^m} \bigg|_{z=\gamma} \frac{d^{N-1-m} g(z, x)}{dz^{N-1-m}} \bigg|_{z=\gamma} \quad (\text{S42})$$

We start by evaluating

$$F_{k_0}(N, m) = \frac{d^m [f(z)]^N}{dz^m} \bigg|_{z=\gamma} = \frac{d^m}{dz^m} \left[\frac{z^2 - a^2}{z + \gamma} \right]^N \bigg|_{z=\gamma}, \quad (\text{S43})$$

where $a = k_0 + i\Gamma(1-2\beta)/2\beta$. In order to compute this we first compute

$$\frac{d^n}{dz^n} \left[\frac{z^2 - a^2}{z + \gamma} \right] \bigg|_{z=\gamma} = (-1)^n n! (2\gamma)^{-n} \left(\frac{\gamma^2 - a^2}{2\gamma} - 2\gamma \delta_{n-1} \right), \quad (\text{S44})$$

where δ_i is the Kronecker delta and takes values $\delta_i = 0$ for $i \neq 0$ and $\delta_i = 1$ for $i = 0$. We can now use Leibniz's rule recursively to express

$$F_{k_0}(N, m) = \sum_{i_1=0}^m \sum_{i_2=0}^{m-i_1} \dots \sum_{i_{N-1}=0}^{m-i_1-i_2-\dots-i_{N-2}} \binom{m}{i_1} \binom{m-i_1}{i_2} \dots \binom{m-i_1-i_2-\dots-i_{N-2}}{i_{N-1}} \times f^{(m-i_1-i_2-\dots-i_{N-1})}(\gamma) \prod_{j=1}^{N-1} f^{(i_j)}(\gamma), \quad (\text{S45})$$

where $f^{(n)}(x_0)$ is the n th derivative of f evaluated at x_0 . We now substitute (S44) into (S45), which, after some manipulation gives

$$\begin{aligned}
F_{k_0}(N, m) &= (-1)^m (2\gamma)^{-m} m! \sum_{i_1}^m \sum_{i_2=0}^{m-i_1} \dots \sum_{i_{N-1}=0}^{m-i_1-i_2-\dots-i_{N-2}} \left[\frac{\gamma^2 - a^2}{2\gamma} - 2\gamma \delta_{i_1-1} \right] \left[\frac{\gamma^2 - a^2}{2\gamma} - 2\gamma \delta_{i_2-1} \right] \\
&\quad \times \dots \times \left[\frac{\gamma^2 - a^2}{2\gamma} - 2\gamma \delta_{i_{N-1}-1} \right] \left[\frac{\gamma^2 - a^2}{2\gamma} - 2\gamma \delta_{m-i_1-i_2-\dots-i_{N-1}-1} \right] \\
&= (-1)^m (2\gamma)^{-m} m! \sum_{i_1}^m \sum_{i_2=0}^{m-i_1} \dots \sum_{i_{N-1}=0}^{m-i_1-i_2-\dots-i_{N-2}} \frac{\gamma^2 - a^2}{2\gamma} \left[\frac{\gamma^2 - a^2}{2\gamma} - 2\gamma \delta_{i_1-1} \right] \left[\frac{\gamma^2 - a^2}{2\gamma} - 2\gamma \delta_{i_2-1} \right] \\
&\quad \times \dots \times \left[\frac{\gamma^2 - a^2}{2\gamma} - 2\gamma \delta_{i_{N-1}-1} \right] \\
&+ (-1)^m (2\gamma)^{-m} m! \sum_{i_1}^m \sum_{i_2=0}^{m-i_1} \dots \sum_{i_{N-1}=0}^{m-i_1-i_2-\dots-i_{N-2}} -2\gamma \delta_{m-i_1-i_2-\dots-i_{N-1}-1} \left[\frac{\gamma^2 - a^2}{2\gamma} - 2\gamma \delta_{i_1-1} \right] \left[\frac{\gamma^2 - a^2}{2\gamma} - 2\gamma \delta_{i_2-1} \right] \\
&\quad \times \dots \times \left[\frac{\gamma^2 - a^2}{2\gamma} - 2\gamma \delta_{i_{N-1}-1} \right], \tag{S46}
\end{aligned}$$

where in the last equality we have split the expression into two terms. These two terms can be written compactly as polynomials using the binomial theorem. We write the first as

$$\frac{\gamma^2 - a^2}{2\gamma} \sum_{k=0}^{N-1} \binom{N-1}{k} \left(\frac{\gamma^2 - a^2}{2\gamma} \right)^{N-1-k} (-1)^k (2\gamma)^k V(N, m, k), \tag{S47}$$

and

$$V(N, m, k) = \sum_{i_1=0}^m \sum_{i_2=0}^{m-i_1} \dots \sum_{i_{N-1}=0}^{m-i_1-i_2-\dots-i_{N-1}} \delta_{i_{x_1}-1} \delta_{i_{x_2}-1} \dots \delta_{i_{x_k}-1}, \tag{S48}$$

where there are k δ factors, and the subscript x_j refers to any of the δ terms when writing the above as a polynomial. Importantly, we can write the form using a binomial expansion only because the value of $V(N, m, k)$ is independent of the subscript of the δ functions and only depends on the total number of them k . We have found that

$$V(N, m, k) = \theta(m-k) \frac{(N-1+m-2k)!}{(m-k)!(N-1-k)!}, \tag{S49}$$

where $\theta(j)$ is the unit step function where $\theta(j) = 1$ for $j \geq 0$ and $\theta(j) = 0$ otherwise, and $m \leq N-1$ and $k \leq N-1$. We can similarly write the second term of (S46) as

$$-2\gamma \sum_{k=0}^{N-1} \binom{N-1}{k} \left(\frac{\gamma^2 - a^2}{2\gamma} \right)^{N-1-k} (-1)^k (2\gamma)^k D(N, m, k), \tag{S50}$$

where

$$\begin{aligned}
D(N, m, k) &= \sum_{i_1=0}^m \sum_{i_2=0}^{m-i_1} \dots \sum_{i_{N-1}=0}^{m-i_1-i_2-\dots-i_{N-1}} \delta_{m-i_1-i_2-\dots-i_{N-1}-1} \delta_{i_{x_1}-1} \delta_{i_{x_2}-1} \dots \delta_{i_{x_k}-1} \\
&= \theta(m-k-1) \frac{(m+N-3-2k)!}{(m-1-k)!(N-k-2)!}, \tag{S51}
\end{aligned}$$

and again we can use this form because the value of the sum only depends on the number of δ factors k . Using (S46) and combining the two terms together we get

$$\begin{aligned}
F_{k_0}(N, m) &= (-1)^m (2\gamma)^{-m} m! \sum_{k=0}^m \frac{N}{N-k} \binom{N-1}{k} \left(\frac{\gamma^2 - a^2}{2\gamma} \right)^{N-k} (-1)^k (2\gamma)^k \frac{(N-1+m-2k)!}{(N-k-1)!(m-k)!} \\
&= (-1)^m (2\gamma)^{-m} \left(\frac{\gamma^2 - a^2}{2\gamma} \right)^N \frac{(N+m-1)!}{(N-1)!} {}_3F_2 \left(\frac{-m, 1-N, -N}{\frac{1-m-N}{2}, \frac{2-m-N}{2}} ; \frac{\gamma^2}{\gamma^2 - a^2} \right), \tag{S52}
\end{aligned}$$

where ${}_3F_2$ is the generalized Hypergeometric function.

We now move to computing the derivative

$$\begin{aligned}
\frac{d^m}{dz^m} \left[\frac{e^{iz|x|}}{z^2 + \Gamma^2/4} \right]_{z=\gamma} &= \frac{e^{i\gamma|x|}}{i\Gamma} \sum_{j=0}^m \binom{m}{j} (i|x|)^{m-j} (-1)^j j! \left[\left(\gamma - \frac{i\Gamma}{2} \right)^{-1-j} - \left(\gamma + \frac{i\Gamma}{2} \right)^{-1-j} \right] \\
&= \frac{1}{i\Gamma} \left\{ e^{\frac{\Gamma}{2}|x|} \left(-\frac{i\Gamma}{2} - \gamma \right)^{-m-1} \Gamma_{m+1} \left[-i \left(\gamma + \frac{i\Gamma}{2} \right) |x| \right] \right. \\
&\quad \left. - e^{-\frac{\Gamma}{2}|x|} \left(\frac{i\Gamma}{2} - \gamma \right)^{-m-1} \Gamma_{m+1} \left[-i \left(\gamma - \frac{i\Gamma}{2} \right) |x| \right] \right\} \\
&\equiv \frac{1}{i\Gamma} \xi_{k_0, m}^{(1)}(x),
\end{aligned} \tag{S53}$$

where $\Gamma_m(x)$ is the incomplete Gamma function. We finally thus have

$$\frac{1}{(N-1)!} \frac{d^{N-1}}{dz^{N-1}} \left[[f(z)]^N g(z, x) \right]_{z=\gamma} = \frac{1}{i\Gamma(N-1)!} \sum_{m=0}^{N-1} \binom{N-1}{m} F_{k_0}(N, m) \xi_{k_0, N-1-m}^{(1)}(x). \tag{S54}$$

The process for evaluating the remaining three differentials is almost identical to the first. The second differential in (S7) is

$$\frac{1}{(N-1)!} \frac{d^{N-1}}{dz^{N-1}} \left[t_{k_0-z}^N (z + k_0 + \frac{i\Gamma}{2\beta} (1-2\beta))^N \frac{e^{-iz|x|}}{z^2 + \Gamma^2/4} \right]_{z=-k_0 - \frac{i\Gamma}{2\beta}} \equiv \frac{1}{(N-1)!} \frac{d^{N-1}}{dz^{N-1}} \left[[f_2(z)]^N g_2(z, x) \right]_{z=-\gamma}, \tag{S55}$$

One can show that

$$\frac{d^m}{dz^m} [f_2(z)]^N \Big|_{z=-\gamma} = (-1)^{(N-m)} F_{k_0}(N, m), \tag{S56}$$

and that

$$\frac{d^m}{dz^m} \left[\frac{e^{-iz|x|}}{z^2 + \Gamma^2/4} \right]_{z=-\gamma} = (-1)^m \frac{1}{i\Gamma} \xi_{k_0, m}^{(1)}(x), \tag{S57}$$

and therefore

$$\frac{1}{(N-1)!} \frac{d^{N-1}}{dz^{N-1}} \left[[f_2(z)]^N g_2(z, x) \right]_{z=-\gamma} = \frac{-1}{i\Gamma(N-1)!} \sum_{m=0}^{N-1} \binom{N-1}{m} F_{k_0}(N, m) \xi_{k_0, N-1-m}^{(1)}(x). \tag{S58}$$

The third differential has the same function raised to the N th power as the first, but the other factor differs, ie.,

$$\frac{1}{(N-1)!} \frac{d^{N-1}}{dz^{N-1}} \left[t_{k_0+z}^N (z - k_0 - \frac{i\Gamma}{2\beta} (1-2\beta))^N \frac{e^{-iz|x|}}{z(z^2 + \Gamma^2/4)} \right]_{z=k_0 + \frac{i\Gamma}{2\beta}} \equiv \frac{1}{(N-1)!} \frac{d^{N-1}}{dz^{N-1}} \left[[f(z)]^N g_3(z, x) \right]_{z=\gamma}. \tag{S59}$$

We therefore are only required to compute

$$\begin{aligned}
\frac{d^m}{dz^m} \left[\frac{e^{-iz|x|}}{z(z^2 + \Gamma^2/4)} \right]_{z=\gamma} &= \frac{e^{i\gamma|x|}}{i\Gamma} \sum_{k=0}^m \binom{m}{k} (i|x|)^{m-k} \frac{d^k}{dz^k} \left[\frac{-1}{z(z+i\Gamma/2)} + \frac{1}{z(z-i\Gamma/2)} \right] \\
&= \frac{e^{i\gamma|x|}}{i\Gamma} \sum_{k=0}^m \binom{m}{k} (i|x|)^{m-k} (-1)^k k! \sum_{l=0}^k \gamma^{l-k-1} \left[\left(\gamma - \frac{i\Gamma}{2} \right)^{-1-l} - \left(\gamma + \frac{i\Gamma}{2} \right)^{-1-l} \right] \\
&= \frac{e^{i\gamma|x|}}{i\Gamma} \sum_{k=0}^m \binom{m}{k} (i|x|)^{m-k} (-1)^k k! \frac{\gamma^{-k-1}}{i\Gamma/2} \left[-2 + \left(\frac{\gamma - i\Gamma/2}{\gamma} \right)^{-k-1} + \left(\frac{\gamma + i\Gamma/2}{\gamma} \right)^{-k-1} \right] \\
&= \frac{1}{\Gamma^2} \left\{ -4(-\gamma)^{-m-1} \Gamma_{m+1}(-i\gamma|x|) + 2e^{-\frac{\Gamma}{2}|x|} \left(-\gamma + \frac{i\Gamma}{2} \right)^{-m-1} \Gamma_{m+1} \left[-i \left(\gamma - \frac{i\Gamma}{2} \right) |x| \right] + \right. \\
&\quad \left. + 2\Gamma_{m+1} \left[-i \left(\gamma + \frac{i\Gamma}{2} \right) |x| \right] \left(-\gamma - \frac{i\Gamma}{2} \right)^{-j-1} e^{\frac{\Gamma}{2}|x|} \right\} \equiv \frac{1}{\Gamma^2} \xi_{k_0, m}^{(3)}(x),
\end{aligned} \tag{S60}$$

and thus

$$\frac{1}{(N-1)!} \frac{d^{N-1}}{dz^{N-1}} \left[[f(z)]^N g_3(z, x) \right]_{z=\gamma} = \frac{1}{\Gamma^2(N-1)!} \sum_{m=0}^{N-1} \binom{N-1}{m} F_{k_0}(N, m) \xi_{k_0, N-1-m}^{(3)}(x). \tag{S61}$$

Finally the fourth differential in (S7) is

$$\frac{1}{(N-1)!} \frac{d^{N-1}}{dz^{N-1}} \left[t_{k_0-z}^N (z + k_0 + \frac{i\Gamma}{2\beta} (1-2\beta))^N \frac{e^{-iz|x|}}{z(z^2 + \Gamma^2/4)} \right]_{z=-k_0 - \frac{i\Gamma}{2\beta}} \equiv \frac{1}{(N-1)!} \frac{d^{N-1}}{dz^{N-1}} \left[[f_2(z)]^N g_4(z, x) \right]_{z=-\gamma}. \tag{S62}$$

One can show that

$$\frac{d^m}{dz^m} \left[\frac{e^{-iz|x|}}{z(z^2 + \Gamma^2/4)} \right]_{z=-\gamma} = \frac{(-1)^{m+1}}{\Gamma^2} \xi_{k_0, m}^{(3)}(x), \tag{S63}$$

and thus

$$\frac{1}{(N-1)!} \frac{d^{N-1}}{dz^{N-1}} \left[[f_2(z)]^N g_4(z, x) \right]_{z=-\gamma} = \frac{1}{\Gamma^2(N-1)!} \sum_{m=0}^{N-1} \binom{N-1}{m} F_{k_0}(N, m) \xi_{k_0, N-1-m}^{(3)}(x). \tag{S64}$$

We can finally combine all four differentials together to get an expression for $\psi_N(x_c, x)$, which after some manipulation yields

$$\psi_N(x_c, x) = e^{2ik_0 x_c} \left\{ t_{k_0}^{2N} - \frac{1}{(N-1)!} \sum_{n=0}^{N-1} \binom{N-1}{n} F_{k_0}(N, n) \chi_{k_0, N-1-n}(x) \right\}, \tag{S65}$$

where

$$\begin{aligned}
\chi_{k_0, n}(x) &= \xi_{k_0, n}^{(1)}(x) - \frac{1}{2} \xi_{k_0, n}^{(3)}(x) \\
&= 2(-\gamma)^{-n-1} \Gamma_{n+1}(-i\gamma|x|) - 2e^{-\frac{\Gamma}{2}|x|} \left(-\gamma + \frac{i\Gamma}{2} \right)^{-n-1} \Gamma_{n+1} \left[-i \left(\gamma - \frac{i\Gamma}{2} \right) |x| \right],
\end{aligned} \tag{S66}$$

giving (S8).